Evolution of the Continents and the Atmosphere Inferred from Th-U-Nb Systematics of the Depleted Mantle

Kenneth D. Collerson* and Balz S. Kamber

Temporal evolution of depleted mantle thorium-uranium-niobium systematics constrain the amount of continental crust present through Earth's history (through the niobium/thorium ratio) and date formation of a globally oxidizing atmosphere and hydrosphere at approximately 2.0 billion years ago (through the niobium/uranium ratio). Increase in the niobium/thorium ratio shows involvement of hydrated lithosphere in differentiation of Earth since approximately 3.8 billion years ago. After approximately 2.0 billion years ago, the decreasing mantle thorium/uranium ratio portrays mainly preferential recycling of uranium in an oxidizing atmosphere and hydrosphere. Net growth rate of continental crust has varied over time, and continents are still growing today.

The nature and time scales of differentiation of Earth's silicate portion into depleted mantle and continental crust, as well as the effects of a changing atmosphere on this process, remain uncertain (*1*). Continental crust is highly enriched in many trace elements. In general, the degree of enrichment follows the order of compatibility (*2*); the most incompatible elements are most strongly enriched in the continents. There are a few prominent exceptions to this rule (Pb, Ti, Nb, and Ta) and we show that the temporal changes in Th, U, and Nb distribution between the continental crust and the depleted mantle (that portion of the mantle from which the continents have been extracted) can be used to reconstruct important aspects of Earth's evolution.

Thorium, U, and Nb behave as strongly incompatible elements during melting of the mantle at midocean ridges (*2*) and have similar bulk distribution coefficients (*3*). Large differences in ratios of Th, U, and Nb between the depleted mantle and the continental crust are therefore not expected. However, continental crust of all ages has a deficit in Nb relative to U and Th, expressed as Nb/U and Nb/Th ratios of <10 and <5, respectively (*4*). These ratios are much lower than those of the undifferentiated, primitive mantle (30 ± 3 and 8 ± 1) (*5*). Depleted mantle has a complementary overabundance of Nb leading to a Nb/U ratio of 44.5 ± 2.5 and a Nb/Th ratio of 18.5 ± 1.2 (*5*). If the temporal evolution of Nb/U and Nb/Th ratios in depleted mantle can be established (*1, 5*), the different behavior of U and Th versus Nb during formation of continental crust can be exploited to infer the mass of continental crust present through geological time.

There is, however, a serious complication in this elegant concept: the present-day Th/U ratio of the depleted mantle is ~2.6 (*6*), which is significantly lower than the time-integrated Th/U value of ~3.75 (*6*) estimated from the Pb isotope composition of midocean-ridge basalts (MORBs). This observation is termed the second terrestrial Pb paradox (*6*). It could either be the result of a temporal change in the Th/U ratio of depleted mantle or a result of recycling of continental Pb (derived from crust with a mean Th/U ratio of ~4.2) back into the mantle. Implication of the first possibility is that the evolution of Nb/U and Nb/Th in depleted mantle would have differed and would therefore not provide an unequivocal estimate of the mass of continental crust present through time.

We estimated the temporal evolution of these ratios, using suites of rocks inferred to be derived from the depleted mantle and ranging in age from 3.8 billion years (Ga) to the present day (Table 1) (*7*). When Th/U ratios of depleted mantle–derived samples are plotted against age (Fig. 1A), the data define a smoothly decaying curve that can be described by a second-order polynomial fit

$$\mathrm{Th/U} = 2.62 + 6.36 \times 10^{-4} \times t - 6.45 \times 10^{-8} \times t^2$$

with $r^2 = 0.989$ and age t in millions of years (Ma). The calculated present-day ($t = 0$) and chondritic values ($t = 4550$ Ma) are 2.55 and 4.18, respectively, in excellent agreement with independently constrained estimates of 2.5 to 2.7 and 3.91 to 4.28 (*8, 9*). The mean time-integrated depleted mantle Th/U ratio obtained from the second-order polynomial fit to the compiled data (Fig. 1A) is 3.4. This value is lower than the Th/U ratio based on the Pb isotope composition of MORB, ~3.75 (*6*). Solution to the second Pb paradox thus involves a mantle with a time-integrated Th/U of 3.4 (as determined above), plus recycling of some continental Pb into the mantle (*9*). In theory, Th and U could have been significantly fractionated during formation of continental crust, in which case the Th/U ratio would portray crustal volume through time. If this were the case, however, the mean age of the resulting continental crust would be younger than 2.0 to 2.2 Ga (*10*). Therefore, evolution of Th/U in the depleted mantle must reflect an additional process. Recycling of continental crust has been suggested as the most likely reason for decoupling of U from Th (*11*). Staudigel *et al.* (*12*) proposed that U would be preferentially recycled into the mantle, but only when the atmosphere and hydrosphere were sufficiently oxidizing

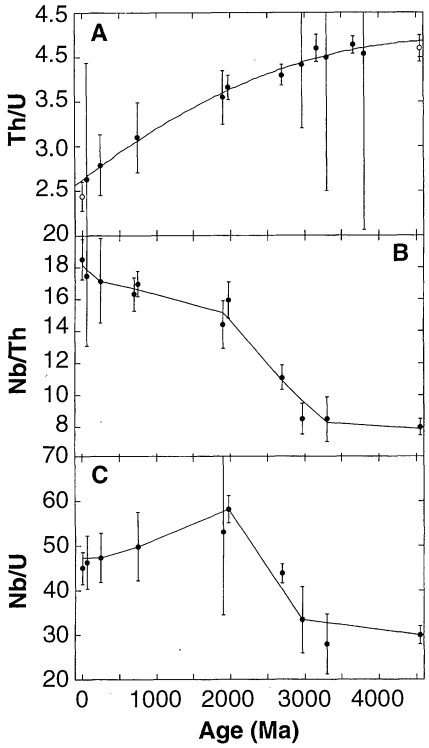

Fig. 1. Evolution of Th, U, and Nb ratios of ancient depleted-mantle–derived rocks from compilation in Table 1. (**A**) Curve for Th/U ratios versus age. Filled circles are data points from Table 1, which were used to obtain a second-order polynomial fit (given in text). Open circles represent target values, which were not included for fit calculation (present-day E-MORB = 2.44 ± 0.16, chondrite average = 4.1 ± 0.1). (**B**) Curve for Nb/Th ratios versus age. All data points are connected by a smoothed interpolation (smoothing factor of 50%). (**C**) Curve for Nb/U ratios versus age. All data points are connected by a smoothed interpolation (smoothing factor 60%). Note the dissimilarity in the behavior of Th and U relative to Nb.

Department of Earth Sciences, The University of Queensland, Brisbane, QLD 4072, Australia. Both authors contributed equally to this publication.

*To whom correspondence should be addressed. E-mail: k.collerson@mailbox.uq.edu.au

to render it mobile. Under present-day oxidizing conditions, Th/U ratios of river waters range between 0.05 and 0.1. This reflects the fact that U is more readily leached from weathered continental crust than is Th, and is mainly transported in dissolved form (*13*). By contrast, Th enters the estuaries as suspended particle load and as a result, the Th/U ratio of seawater is even lower than that of river water (*13*). Under an oxidizing atmosphere U is preferentially transported into the open ocean where it is incorporated into marine sediments and altered oceanic crust, which are eventually subducted.

In the mantle samples, the temporal evolution of Nb/Th and Nb/U ratios differ (Fig. 1, B and C). The Nb/Th ratio generally increased with time, slowly between the present day and ~2 Ga, strongly between 2 and 3.5 Ga, and very slowly during earliest Earth history. This contrasts with the Nb/U ratio, which increased slowly during the early and middle Archaean and then strongly during late Archaean and early Proterozoic to a maximum value of ~58 at 2.0 Ga. The Nb/U ratio then decreased to the present-day value of 44.5.

Thus, the Nb/U and Nb/Th ratios in depleted mantle both evolved to significantly higher values than those of primitive mantle. There are two plausible mechanisms capable of efficiently fractionating Nb from U and Th. (i) The presence of rutile, a stable phase in the eclogite assemblage formed by subduction of oceanic crust, significantly changes the bulk distribution coefficient for Nb (*14*) because Nb substitutes for Ti. Thus, melt in equilibrium with rutile has a Nb deficit relative to U and Th. (ii) Dehydration of the subducting slab leads to depletion of the oceanic crust in some elements (for example U, Th, and Rb), which are transported to the melting environment of the overlying mantle wedge. The degree of depletion depends on the distribution coefficients between the eclogite assemblage and fluid (not melt). Uranium and Th are significantly more mobile than Nb, and thus the fluid will be characterized by low Nb/U and Nb/Th ratios (*14*). This indicates that growth of continental crust must have, at least in part, involved subduction zone–induced melting.

The Nb/U and Nb/Th curves can be converted to curves of crust volume versus age (CvA curves) by assuming that there was 0% crust present for chondritic values and 100% crust present for the present-day MORB values. However, these two proxies yield very different topologies (Fig. 2A). The CvA curve based on Nb/Th ratio agrees well with independent CvA estimates (Fig. 2B): the post-Archaean CvA curve of Reymer and Schubert (*15*), which is based on geophysical considerations, and the CvA curve of Kramers and Tolstikhin (*9*), which satisfies both terrestrial Pb paradoxes as well as the Nd isotope database (*16*). We therefore combined these three proxies to yield a new composite CvA curve (solid line in Fig. 2B).

In contrast, if the Nb/U ratio is converted into a CvA curve (Fig. 2A), using the approach described above, it predicts that late Archaean to early Proterozoic continental crust was volumetrically similar (*1*), if not more voluminous than continental crust today (*17*). This hypothesis of constant, or even decreasing, crustal volume since the late Archaean is not supported by other constraints: (i) it is not recorded in the estimated Nd isotope evolution of depleted mantle (*16*); (ii) it fails to account for the observed crustal age distribution (*10*); and (iii) the required high recycling rates (comparable to, or greater than, estimated production rates of ~1 $km^3\ a^{-1}$) would erase the future Pb paradox (*9, 11*).

The Nb/U ratio of the depleted mantle therefore not only reflects the volume of con-

Table 1. Compilation of Th, U, and Nb data for depleted mantle–derived rocks (error = 1 SD). ε_{Nd} expresses the fractional difference between the initial $^{143}Nd/^{144}Nd$ ratio of the rocks and the corresponding value of this ratio in the chondritic uniform reservoir at the time of crystallization of the rocks, expressed in units of 10^4. Fm., formation.

Age (Ma)	Rock type	Location	ε_{Nd}	Th/U ± SD	Nb/U ± SD	Nb/Th ± SD	Data source
0	E-MORB	East Pacific	~10	2.44 ± 0.16	45.07 ± 3.55	18.5 ± 1.25	(*7*)
30–90	MORB	Indian, Pacific	~9	2.63 ± 1.31	46.35 ± 5.9	17.50 ± 4.42	(*19*)
240	Pillow basalt	Pioneer Fm.		2.79 ± 0.34	47.35 ± 5.52	17.16 ± 2.66	(*20*)
700	Basalt	Avalon arc	~4.7			16.33 ± 1.05	(*21*)
750	Meta-basalt	Ogcheon belt	~4.5			17.69 ± 3.9	(*22*)
750	Basalt dyke	Tilemsi belt		3.38 ± 0.49	55.32 ± 12.01	16.45 ± 3.51	(*23*)
750	Basalt	Gabal-Gerf	~8	2.83 ± 0.63	44.44 ± 11.73	16.11 ± 2.00	(*24*)
750	Gabbro	Gabal-Gerf				17.63 ± 2.86	(*24*)
750	Average*			3.10 ± 0.39	49.88 ± 7.69	16.97 ± 0.81	(22–24)
1900	Basalt	Flin-Flon	~4	3.34 ± 0.41	52.99 ± 18.43	14.48 ± 2.99	(*25*)
1900	Basalt	Flin-Flon		3.77 ± 0.25			(*26*)
1900	Basalt	Flin-Flon				12.77 ± 3.89	(*27*)
1900	Basalt dyke	Joruma				15.35 ± 3.23	(*28*)
1900	Pillow lava	Joruma				13.67 ± 3.54	(*28*)
1900	Average*			3.55 ± 0.3	52.99 ± 18.43	14.40 ± 1.50	(25–28)
1980	Basalt	Onega	~3	3.66 ± 0.14	58.26 ± 3.08	15.94 ± 1.13	(*17*)
2700	Spinifex komatiite	Abitibi	2.5	4.17 ± 1.10	47.80 ± 6.37	11.96 ± 2.59	(*29*)
2700	Komatiite + basalt	Abitibi		3.94 ± 0.97	46.82 ± 15.41	11.93 ± 2.61	(*30*)
2710	Komatiite + basalt	Abitibi				11.14 ± 1.33	(*31*)
2710	Basalt, borehole1	Lunnon Fm.	~2.5	3.75 ± 0.15	43.87 ± 2.71	11.72 ± 0.97	(*1*)
2710	Basalt, borehole 2	Lunnon Fm.		3.86 ± 0.20	39.61 ± 6.09	10.23 ± 1.28	(*1*)
2720	Komatiite + basalt	Abitibi	~3			11.82 ± 1.75	(*32*)
2730	Mafic + ultramafic	Superior		4.58 ± 1.22	43.99 ± 10.56	9.74 ± 1.52	(*33*)
2700	Average*			3.80 ± 0.12	43.80 ± 2.20	11.11 ± 0.79	(*1, 29–33*)
2970	Basalt + komatiite	Superior		3.92 ± 0.72	33.45 ± 7.41	8.51 ± 0.96	(*34*)
3170	Basalt + komatiite	Barberton		4.11 ± 0.15			(*35*)
~3300	Basalt	Pilbara				8.92 ± 3.94	(*36*)
~3300	Spinifex komatiite	Barberton	~2	5.55 ± 0.90	48.21 ± 14.12	8.79 ± 2.63	(*29*)
~3300	Komatiite	Barberton		2.59 ± 0.61	21.75 ± 7.83	8.29 ± 1.87	(*5*)
3300	Average*			4.00 ± 1.50	28.00 ± 6.70	8.50 ± 1.40	(*5, 29, 36*)
3650	Tonalite	SW-Greenland	1	4.14 ± 0.10			(*37*)
3800	Meta-komatiite	Labrador		4.04 ± 1.98			(*38*)

*Averages are of all preceding data with the same age. The 2700 average is from data at 2700, 2710, 2720, and 2730 Ma.

tinental crust, it is also influenced by the preferential recycling of U (over Th and Nb). The kink in the Nb/U evolution (Fig. 1C) dates the time of formation of an atmosphere and hydrosphere that were sufficiently oxidizing to allow U transport in the form of UO_2^{2+} (*11, 12*). This interpretation is supported by the observation that the Th/U ratio in cratonic shales increased from ~3.5 in the Archaean to ~4.2 in the Proterozoic and ~4.6 in the Phanerozoic in spite of a relatively constant upper-crustal Th/U ratio through time (*4*).

The evolution of Th/U in depleted mantle can be quantitatively assessed using the constraints derived from Nb/Th and Nb/U systematics. The evolution of the Th/U ratio between ~3.8 and 2.0 Ga is interpreted to be solely a result of extraction of continental crust. The strong decrease in Th/U ratio after 2.0 Ga is interpreted to result from preferential U recycling, superimposed on extraction of more continental crust. From our parameterization of the CvA curve, a hypothetical Th/U evolution of the depleted mantle can be calculated by equating the evolution from a chondritic value of 4.18 with 0% continental crust and the Th/U ratio at 2.0 Ga of 3.64 with ~67% continental crust present (Fig. 3). This model represents the Th/U evolution of depleted mantle in a permanently anoxic Earth. The observed Th/U ratio and the predicted ratio, based on crust volume alone, show agreement between 4.55 and 2.0 Ga; however, the curves deviate between 2 Ga and the present day. If the hypothetical Th/U curve is calculated with an anchor point outside 1.8 to 2.2 Ga, the fit worsens rapidly in the section before 2.0 Ga. We therefore conclude that this age range (1.8 to 2.2 Ga) reflects timing of development of a pandemic oxidizing atmosphere. This is supported by the recent discovery of laterites 2.0 to 2.2 Ga in age and by cessation of deposition of banded-iron formation (*18*).

This model can be independently tested with Pb isotope systematics of upper continental crust. To satisfy mass-balance considerations (using a chondrite ratio of 4.1 and a present-day depleted-mantle ratio of 2.55), the mean Th/U ratio of present-day continental crust must be ~4.5. The hypothetical Th/U evolution of an anoxic Earth predicts that the mean continental crustal Th/U ratio was lower (<4.25) between 4.55 and 2.0 Ga. The inescapable implication (which is independent of exact Th/U ratios) is that the Th/U ratio of the continental crust has increased between 2.0 Ga and the present day. Our model is strengthened by the observation that post-Archaean samples of upper crust show the predicted increase in initial $^{208}Pb/^{206}Pb$ isotope ratios (*9*).

The observed present-day depleted mantle is enriched in U by ~30% compared to the hypothetical mantle in an anoxic Earth (with no preferential U recycling; Fig. 3). The U required for this surplus corresponds to only ~6% of that hosted in continental crust. The amount of U eventually recycled into the depleted mantle therefore only represents a small fraction of the total U budget that entered the oceans (and eventually marine sediments and hydrated oceanic lithosphere). Calculation of a reliable crustal recycling rate from the difference in U concentration between the observed and the modeled depleted mantle is not possible, because U is highly mobile and incompatible during subduction zone dehydration (*14*). Nevertheless, an important feature of the observed Th/U evolution of the depleted mantle (Fig. 3) is that continental recycling increased a few hundred million years after the onset of formation of a globally oxidizing atmosphere. This pattern indicates that an increase in the level of free oxygen in the atmosphere accelerates the rate of continental recycling (erosion rates). Although the cause of this phenomenon is unknown, it is possible that a change in subaerial biological activity could have played a major role in enhancing continental weathering (*16, 18*).

Continental growth rate has varied substantially over geological time. Strong net growth is recorded between 3.0 and 2.0 Ga, but generally slowed down after 2.0 Ga due to increased erosion. Superimposed on this pattern is the effect of Proterozoic supercontinent assembly (Nena, Rodinia, Gondwana) resulting in small total continental circumference, and hence, decreased total subduction melt flux at that time. Renewed increase of net crustal growth from ~250 Ma to the present day indicates faster continental growth during times of continental dispersal.

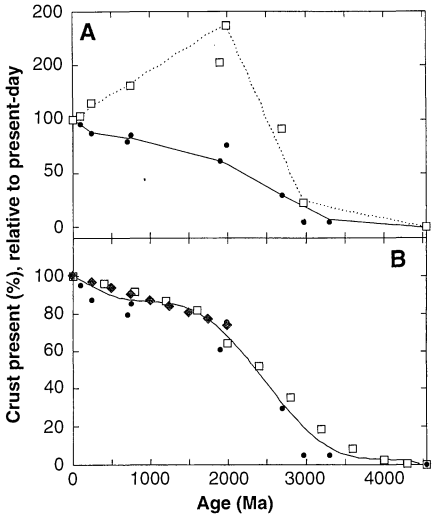

Fig. 2. Curves for crust volume versus age. (**A**) Comparison of crust volumes estimated through the Nb/Th ratio (filled circles, connected by solid line) and through the Nb/U ratio (open squares, connected by dotted line). Estimation is based on the assumption that the chondritic values represent 0% crust and that present-day MORB average represents 100% of present continental crust volume. Note that the Nb/U-based estimate predicts the former existence of a substantially more voluminous continental crust. (**B**) Comparison of crust volumes estimated from geophysical data by Reymer and Schubert (*15*) (solid diamonds), transport-forward modeling by Kramers and Tolstikhin (*9*) (open squares), and the Nb/Th evolution of the depleted mantle in (A) (solid circles). Solid line represents composite parameterization for the crust volume versus age (eight data points from Reymer and Schubert, 12 data points from Kramers and Tolstikhin, and all 10 Nb/Th data points). Relative to the present-day volume or mass of continental crust, the percent volume or mass of continental crust (y) present at any given age (t, in megannum) can be expressed as a seven-order polynomial: $y = 100 - 1.5742 \times 10^{-2} \times t - 4.2617 \times 10^{-5} \times t^2 + 9.9543 \times 10^{-8} \times t^3 - 7.663 \times 10^{-11} \times t^4 + 2.5738 \times 10^{-14} \times t^5 - 3.9626 \times 10^{-18} \times t^6 + 2.3005 \times 10^{-22} \times t^7$ with $r^2 = 0.984$.

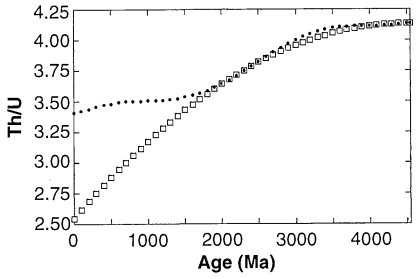

Fig. 3. Comparison of the evolution of the observed Th/U ratio (open squares, approximated by a second-order polynomial fit; Fig. 1) with a hypothetical Th/U ratio in an anoxic Earth (solid circles, where no preferential U recycling was possible). The hypothetical evolution is calculated assuming that the decrease of the Th/U ratio in the depleted mantle is purely due to extraction of continental crust (discussed in text).

References and Notes

1. P. J. Sylvester, I. H. Campbell, D. A. Bowyer, *Science* **275**, 521 (1997); R. L. Armstrong, *Philos. Trans. R. Soc. London Ser. A* **301**, 443 (1981).
2. During partial melting of the mantle, incompatible elements partition preferentially into the melt [A. W. Hofmann, *Earth Planet. Sci. Lett.* **90**, 297 (1988)].
3. For relatively high melt fractions (for example, melt generation at midocean ridges), the bulk distribution coefficients for Th, U, and Nb are very similar. Hence, the ratios between these elements in melt products are similar to those in the source.
4. K. C. Condie, *Chem. Geol.* **104**, 1 (1993).
5. A. W. Hofmann, K. P. Jochum, M. Seufert, W. M. White, *Earth Planet. Sci. Lett.* **79**, 33 (1986); K. P. Jochum, N. T. Arndt, A. W. Hofmann, *ibid.* **107**, 272 (1991).
6. S. J. G. Galer and R. K. O'Nions, *Nature* **316**, 778 (1985).
7. Table 1 was compiled from trace-element datasets obtained by inductively coupled plasma mass spectrometry and spark-source mass spectrometry. All selected samples have been interpreted to be derived from depleted mantle by the original authors. Because U and Th occur in low concentrations in mantle melts, even minor contamination of these melts with crustal or lithospheric mantle material (in which Th and U are more abundant or can be strongly fractionated, or both) is a concern. Therefore, we concentrated on trace-element datasets that apparently have not been affected by crustal contamination by selecting only samples

that yield consistent and radiogenic initial Nd isotope ratios and trace-element patterns characteristic of mid-ocean ridge melts. Other selection criteria include using trace-element data for rocks with high MgO (>6 wt%) to eliminate the possibility of oxide-induced fractionation of Nb versus Th and U [Y. Niu, K. D. Collerson, R. Batiza, J. I. Wendt, M. Regelous, *J. Geophys. Res.*, in press] and using suites believed to be of volcanic origin (rather than cumulates) to avoid Th/U fractionation caused by crystallization processes. From these criteria, the best datasets are derived from uncontaminated Archaean to early Proterozoic komatiites, komatiitic basalts, and basalts; post-Archaean obducted normal (N-MORB) or enriched (E-MORB) MORB ophiolites; tectonically emplaced intraoceanic arcs; and some uncontaminated continental mafic volcanics (Table 1). Three Th/U ratios were also calculated from initial $^{208}Pb/^{204}Pb$ and $^{206}Pb/^{204}Pb$ isotope data of other mantle-derived rocks. The standard deviations of most individual datasets are between ~5 and 10%. This is significantly smaller than the total variation in the ratio over geological time. The means of individual datasets of the same age are in excellent agreement (Table 1). Because we compare relative changes of elemental ratios, our conclusions are not impaired by the slight differences in the bulk distribution coefficients of the three elements.

8. C. J. Allègre and E. Lewin, *Earth Planet. Sci. Lett.* **96**, 61 (1989).
9. J. D. Kramers and I. N. Tolstikhin, *Chem. Geol.* **139**, 75 (1997).
10. The mean Nd isotope mantle extraction age of continental crust is between 2.0 and 2.2 Ga [S. R. Taylor and S. M. McLennan, *Rev. Geophys.* **33**, 241 (1995); S. L. Goldstein, R. K. O'Nions, P. J. Hamilton, *Earth Planet. Sci. Lett.* **70**, 221 (1984)].
11. I. J. Duncan, *J. Geodyn.* **2**, 1 (1985); R. E. Zartman and S. Haines, *Geochim. Cosmochim. Acta* **52**, 1327 (1988); M. T. McCulloch, *Earth Planet. Sci. Lett.* **115**, 89 (1993).
12. H. Staudigel, G. R. Davies, S. R. Hart, K. M. Marchant, B. M. Smith, *Earth Planet. Sci. Lett.* **130**, 169 (1995).
13. Y. Asmerom and S. B. Jacobsen, *ibid.* **115**, 245 (1993); P. S. Andersson, G. J. Wasserburg, J. H. Chen, D. A. Papanastassiou, J. Ingri, *ibid.* **130**, 217 (1995); D. Mathieu, M. Bernat, D. Nahon, *ibid.* **136**, 703 (1995).
14. R. Stalder, S. F. Foley, G. P. Brey, I. Horn, *Geochim. Cosmochim. Acta* **62**, 1781 (1998); J. M. Brenan, H. F. Shaw, D. L. Phinney, F. J. Ryerson, *Earth Planet. Sci. Lett.* **128**, 327 (1994); J. Ayers, *Contrib. Mineral. Petrol.* **132**, 390 (1998).
15. A. Reymer and G. Schubert, *Tectonics* **3**, 63 (1984).
16. J. D. Kramers, T. F. Nägler, I. N. Tolstikhin, *Schweiz. Mineral. Petrogr. Mitt.* **78**, 169 (1998); T. F. Nägler and J. D. Kramers, *Precambrian Res.* **91**, 233 (1998).
17. Averages of Angozero suite [I. S. Puchtel *et al.*, *Contrib. Mineral. Petrol.* **130**, 134 (1998)] quoted in Table 1 omitted samples 89103 and 9112 because of aberrant Th/U ratios.
18. J. Gutzmer and N. J. Beukes, *Geology* **26**, 263 (1998); A. E. Isley, *J. Geol.* **103**, 169 (1995).
19. Average of Deep Sea Drilling Project Legs 28 and 29 is from D. G. Pyle, D. M. Christie, J. J. Mahoney, and R. A. Duncan [*J. Geophys. Res.* **100**, 22261 (1995)]. The Th/U data is from old Western Indian Ocean [J. J. Mahoney *et al.*, *J. Petrol.* **39**, 1285 (1998)].
20. J. Dostal and B. N. Church, *Geol. Mag.* **131**, 243 (1994).
21. J. D. Keppie and J. Dostal, *ibid.* **135**, 171 (1998). Sample 191A was rejected due to high Th concentration.
22. K. S. Lee, H. W. Chang, K. H. Park, *Precambrian Res.* **89**, 47 (1998).
23. Average of dyke complex samples is from J. Dostal, C. Dupuy, and R. Caby [*ibid.* **65**, 55 (1994)].
24. M. Zimmer, A. Kröner, K. P. Jochum, T. Reischmann, W. Todt, *Chem. Geol.* **123**, 29 (1995). Basalt average was calculated without samples GG72, GG184, and GG172, for which U disturbance is inferred; gabbro average was calculated from samples GG77, GG82, GG87, and GG88 (only used for Nb/Th ratios).
25. Average of E-MORB is from R. A. Stern, E. C. Syme, and S. B. Lucas [*Geochim. Cosmochim. Acta* **59**, 3131 (1995)].
26. The Th/U ratio was calculated from Pb isotope systematics [N. T. Arndt and W. Todt, *Chem. Geol.* **118**, 9 (1994)].
27. Average of transitional basalts with Th concentration lower than 0.35 ppm is from M. I. Leybourne, N. A. van Wagoner, and L. D. Ayres [*J. Petrol.* **38**, 1541 (1997)].
28. P. Peltonen, A. Kontinen, H. Huhma, *ibid.* **37**, 1359 (1996).
29. Averages of spinifex textured komatiites for Abitibi and Barberton are from Y. Lahaye *et al.* [*Chem. Geol.* **126**, 43 (1995)].
30. Average of komatiite, spinifex-komatiite, and komatiitic basalt is from J. Fan and R. Kerrich [*Geochim. Cosmochim. Acta* **61**, 4723 (1997)].
31. Average of komatiites and Fe basalts is from Q. Xie, R. Kerrich, and J. Fan [*ibid.* **57**, 4111 (1993)].
32. Average of komatiites and basalts is from J. Dostal and W. U. Mueller [*J. Geol.* **105**, 545 (1997)].
33. J. A. Ayer and D. W. Davis, *Precambrian Res.* **81**, 155 (1997). Only least-contaminated samples 84-610, 93-22, 89-110, 87-838, and 87-839 from lower Keewatin were used.
34. Average of all komatiites and basalts is from K. Y. Tomlinson *et al.* [*ibid.* **89**, 59 (1998)]. Sample KYT376 was rejected due to high Th concentration (1.61 ppm).
35. Time-integrated Th/U ratio based on Pb isotopes is from A. H. Wilson and R. W. Carlson [*Earth Planet. Sci. Lett*, **96**, 89 (1989)].
36. Average of Archean-MORB basalts is from H. Ohta, S. Maruyama, E. Takahashi, Y. Watanabe, and Y. Kato [*Lithos* **37**, 199 (1996)]. Samples CLG-10 and CLG-12.H were excluded.
37. B. S. Kamber and S. Moorbath, *Chem. Geol.* **150**, 19 (1998). The Th/U ratio of depleted mantle is derived from least-radiogenic silicate Pb isotope ratios on Earth.
38. K. D. Collerson, unpublished data.
39. This work could not have been done without the high-quality datasets published by our colleagues. Research on crustal evolution by K.D.C. was supported by NSF and the Australian Research Council. B.S.K. is funded by Swiss National Science Foundation grant 8220-050352.

2 November 1998; accepted 25 January 1999

Rapid Thinning of Parts of the Southern Greenland Ice Sheet

W. Krabill,[1]* E. Frederick,[2] S. Manizade,[2] C. Martin,[2] J. Sonntag,[2] R. Swift,[2] R. Thomas,[2] W. Wright,[1] J. Yungel[2]

Aircraft laser-altimeter surveys over southern Greenland in 1993 and 1998 show three areas of thickening by more than 10 centimeters per year in the southern part of the region and large areas of thinning, particularly in the east. Above 2000 meters elevation the ice sheet is in balance but thinning predominates at lower elevations, with rates exceeding 1 meter per year on east coast outlet glaciers. These high thinning rates occur at different latitudes and at elevations up to 1500 meters, which suggests that they are caused by increased rates of creep thinning rather than by excessive melting. Taken as a whole, the surveyed region is in negative balance.

The mass balance of the polar ice sheets is clearly important to global sea level, but it is still not known whether the Greenland and Antarctic ice sheets are increasing or decreasing in size. Mass balance can be inferred directly by comparing repeated aircraft or satellite altimeter surveys over periods of a few years, giving an indication of the change in volume over the survey intervals. Recent analyses of Seasat and Geosat radar-altimeter data over southern Greenland (*1*) indicate average thickening between 2 and 4 cm/year at elevations above 2000 and 1700 m, respectively, for the period 1978–1988 at latitudes less than 72°N. Because of limitations associated with the satellite instruments, there are few useful data below elevations of 2000 m and scarcely any below 1700 m. Here, we present results from aircraft laser-altimeter measurements of elevation change over all of southern Greenland, including first estimates for the peripheral regions, which represent about 40% of the ice sheet area and are likely to be most susceptible to climate change.

In 1993 and 1994, NASA surveyed the entire Greenland ice sheet by airborne laser altimetry, obtaining surface-elevation profiles with root mean square (rms) accuracy of 10 cm or better (*2*) along flight lines that crossed all the major catchment basins. In 1998, the 10 flight lines flown in 1993 in the south of Greenland were resurveyed with about 99% repeat coverage; the flight lines in the north will be resurveyed in 1999.

The airborne topographic mapper (ATM) is a conical-scanning laser ranging system with a pulse repetition rate of 3 kHz (800 Hz in 1993) and a scan rate of 10 Hz (5 Hz), at an off-nadir angle of 10°. Aircraft location was determined by kinematic global positioning system (GPS) techniques, and aircraft heading, pitch, and roll were measured by inertial navigation systems. At an aircraft altitude of 400 m above the surface, the ATM obtained measurements of the surface elevations for many 1-m footprints within a 140-m-wide swath, with average sep-

[1] Laboratory for Hydrospheric Processes, NASA Goddard Space Flight Center, Wallops Flight Facility, Building N-159, Wallops Island, VA 23337, USA. [2]EG&G Services, Wallops Flight Facility, Building N-159, Wallops Island, VA 23337, USA.

*To whom correspondence should be addressed. E-mail: krabill@osb.wff.nasa.gov